Original Research

SPINE RESEARCH

OPEN

A novel X-ray-based screening model for bilateral L5 spondylolysis

Chuncheung Chan[a], Xiaojie Liu[a], Dacheng He[a], Hongfei Xiang[b], Jiyu Li[c], Fuxin Wei[a,*]

Abstract

Background: Lumbar spondylolysis is commonly evaluated initially with lumbar radiography, but radiographs may miss pars interarticularis defects, particularly at L5. This study aimed to characterize radiographic and morphological features associated with bilateral L5 spondylolysis and to develop and externally evaluate an X-ray-based screening nomogram for radiographic risk stratification.

Methods: This cross-sectional study included patients who underwent lumbar radiography and computed tomography (CT) between 2018 and 2025. Patients with CT-confirmed bilateral L5 spondylolysis were compared with controls without spondylolysis. Radiographic parameters and CT-based morphological features were measured and analyzed separately, and interobserver reliability was assessed. Propensity score matching (PSM) (1:1) was used to balance baseline characteristics. Factors associated with L5 spondylolysis were identified using multivariable logistic regression, and an X-ray-only nomogram was constructed using significant radiographic variables. Model performance in the development cohort was assessed using discrimination, calibration, decision curve analysis (DCA), and clinical impact curves (CICs) with internal bootstrap validation. External validation applied the original development-cohort coefficients without refitting and primarily assessed discrimination in an independent dataset.

Results: After PSM, 114 patients were included in the development cohort, with 57 patients in each group. Compared with controls, patients with L5 spondylolysis had larger sacral slope (SS), L5 lamina inclination angle (L5 LIA), and pedicle internal inclination angle, as well as smaller sacral inclination (SI) and L5 lumbar index. Multivariable analysis identified smaller SI, smaller L5 lumbar index, larger SS, larger L5 LIA, and larger pedicle internal inclination angle as factors independently associated with L5 spondylolysis. L5 LIA showed the strongest individual diagnostic performance (area under the curve [AUC] = 0.879; 95% CI, 0.813–0.944). The X-ray screening model incorporating the L5 lumbar index, SI, SS, and L5 LIA achieved excellent discrimination in the development cohort (AUC = 0.916; bootstrap-corrected concordance index = 0.911) and maintained strong discrimination in the external validation dataset when the development-cohort coefficients were applied without refitting (AUC/C-index = 0.949; 95% CI, 0.922–0.977).

Conclusions: An X-ray-based nomogram incorporating key sagittal alignment and morphological parameters showed strong diagnostic discrimination for bilateral L5 spondylolysis in both the development cohort and the external validation dataset. This model should be interpreted as a radiographic screening and risk-stratification aid rather than a tool for prospective prognosis. CT-based analysis also showed that patients with L5 spondylolysis had a larger pedicle internal inclination angle, a morphological difference with potential relevance to preoperative planning.

Abbreviation: CIC = clinical impact curve, DCA = decision curve analysis, IJS = intervertebral joint space, LIA = lamina inclination angle, PSM = propensity score matching, ROC = receiver operating characteristic, SI = sacral inclination angle, SS = sacral slope angle.

Keywords: lumbar vertebrae, nomograms, radiography, spondylolysis, tomography, X-ray computed

1. Introduction

Lumbar spondylolysis is a bony defect located between the posterior elements of the vertebral body and the

CC and XL contributed equally to this article.

[a] Department of Spine, The Seventh Affiliated Hospital, Sun Yat-sen University, Shenzhen, China, [b] Department of Spine Surgery, The Affiliated Hospital of Qingdao University, Qingdao, China, [c] School of Biomedical Engineering, Shenzhen Campus of Sun Yat-sen University, Shenzhen, China

* Correspondence: Fuxin Wei, MD, Department of Spine, The Seventh Affiliated Hospital, Sun Yat-sen University, No. 628, Zhenyuan Road, Shenzhen 518000, China (e-mail: weifuxin@mail.sysu.edu.cn).

© The Author(s) 2026. Published by Wolters Kluwer Health, LLC. on behalf of Higher Education Press. This is an open access article distributed under the Creative Commons Attribution License 4.0 (CCBY), which permits unrestricted use, distribution, and reproduction in any medium, provided the original work is properly cited.

Spine Research (2026) 2:3;173–182

Received: 3 May 2026 / Accepted: 18 June 2026

Published online 9 July 2026

http://dx.doi.org/10.1097/br9.0000000000000039

articular processes and is typically bridged by fibrous, cartilaginous, or osseous tissue.[1,2] Approximately 80% of individuals with lumbar spondylolysis remain asymptomatic, and the condition is often identified incidentally or during postmortem examinations; when symptoms occur, low back pain is the predominant clinical manifestation.[3,4] Epidemiological studies have reported an overall prevalence of approximately 6% in the general population, with most estimates ranging from 3% to 10%.[5,6] The incidence varies substantially across ethnic groups and occupational populations, reaching up to 50% among Inuit populations and between 11.0% and 52.6% in young athletes.[7,8]

The L5 vertebra is the most frequently affected level, accounting for more than 90% of reported cases.[9,10] When bilateral spondylolysis occurs at L5, approximately 70% of patients subsequently develop lumbar spondylolisthesis, underscoring the clinical importance of early and accurate diagnosis.[11]

In routine practice, lumbar radiography, including anteroposterior, lateral, and dynamic views, remains the most commonly used initial imaging modality for suspected lumbar spondylolysis.[12,13] However, its diagnostic accuracy is often compromised by facet joint hypertrophy and obscuration by the iliac crest, particularly at the L5 level, which can lead to missed or delayed diagnosis.[14] Computed tomography (CT), which provides multiplanar visualization in coronal, sagittal, and axial planes, is widely regarded as the diagnostic reference standard.[1] Nevertheless, CT is associated with relatively high radiation exposure, longer examination times, and increased cost.[15]

In clinical practice, patients with L5 spondylolysis often appear to require a greater pedicle screw insertion angle during surgical fixation, suggesting the presence of distinct morphological characteristics. Therefore, this study aimed to elucidate radiographic and morphological features associated with bilateral L5 spondylolysis and to develop an X-ray-based screening model capable of improving radiographic risk stratification and supporting decisions regarding further CT evaluation.

2. Methods

2.1. Study design and patient selection

This cross-sectional diagnostic screening study systematically analyzed patients hospitalized between 2018 and 2025. The study was reported in accordance with relevant observational and diagnostic-accuracy reporting principles where applicable.

The inclusion criteria were as follows: availability of lumbar spine radiographs, including anteroposterior, lateral, and dynamic views; and completion of lumbar CT examination. The exclusion criteria were as follows: non-L5 spondylolysis; rheumatoid or immune-related disease; history of malignancy; multilevel spondylolysis or unilateral L5 spondylolysis; spinal scoliosis, infection, or previous fracture; prior lumbar surgery; and age younger than 18 years.

Patients with unilateral L5 spondylolysis, multilevel spondylolysis, or non-L5 defects were excluded to maintain a morphologically homogeneous bilateral L5 cohort. Defect laterality and involved vertebral level may have different biomechanical patterns and radiographic manifestations; therefore, the resulting model was intended for bilateral L5 spondylolysis and should not be directly generalized to unilateral or multilevel disease.

Based on CT findings, patients were classified into two groups. Individuals with CT-confirmed defects of the pars interarticularis were assigned to the spondylolysis group, whereas those without such defects were classified as controls.

2.2. Ethics approval and consent to participate

This study was approved by the Institutional Review Board and Ethics Committee of The Seventh Affiliated Hospital, Sun Yat-sen University, Shenzhen, China (Approval No. KY-2025-563-01, Date: December 10, 2025). The requirement for informed consent was waived by the Medical Ethics Committee of the Seventh Affiliated Hospital of Sun Yat-sen University. All procedures were conducted in accordance with applicable institutional guidelines and the Declaration of Helsinki.

2.3. Data collection and imaging measurements

Demographic variables included age, sex, body mass index (BMI), and histories of diabetes mellitus and hypertension.

Radiographic parameters measured on lumbar X-rays are illustrated in Figure 1 and included intervertebral joint space (IJS) on the anteroposterior view, lamina inclination angle (LIA) on the lateral view, sacral inclination angle (SI), sacral slope angle (SS), L5 lumbar index (a/b ratio), degree of spondylolisthesis, and lumbar instability when assessable on dynamic radiographs. The candidate variables for the X-ray screening model were restricted to parameters obtainable from standard radiographs.

CT-based parameters were measured using the Magerl method and included the presence of L5 spondylolysis, pedicle width, intended screw depth, and pedicle internal inclination angle (Fig. 2).[16] These CT-based variables were analyzed as morphological and surgically relevant features but were not included in the final X-ray-only screening nomogram.

All measurements were independently performed by two observers, with repeated measurements obtained at a 1-week interval. Measurement reliability was assessed using intraclass correlation coefficients (ICCs).[17] ICC values greater than 0.75 were considered indicative of good reproducibility.[18]

2.4. Propensity score matching

To minimize confounding, 1:1 propensity score matching (PSM) was performed.[19] Propensity scores were

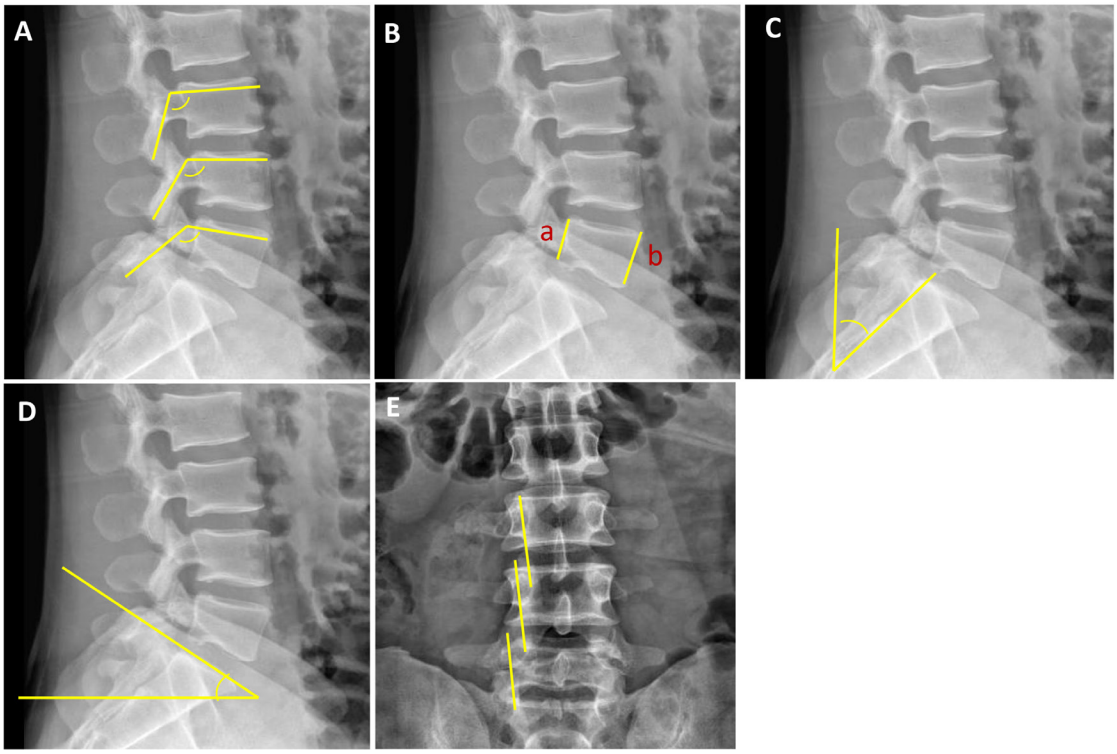


Figure 1. Radiographic measurements on lumbar radiographs. (A) Lamina inclination angle (LIA). (B) L5 lumbar index (a/b). (C) Sacral inclination angle (SI). (D) Sacral slope angle (SS). (E) Intervertebral joint space (IJS).

calculated using logistic regression models incorporating age, sex, BMI, diabetes mellitus, and hypertension. Matching was conducted with a caliper width of 20% of the standard deviation of the propensity score, with random selection among individuals sharing identical scores.[20]

2.5. Statistical analysis

Continuous variables were analyzed using Student's *t* test or the Wilcoxon rank-sum test, as appropriate. Categorical variables were compared using the chi-square test. Variables significant in univariable analysis were entered into multivariable logistic regression models. Model discrimination was evaluated using receiver operating characteristic (ROC) curves and the area under the curve (AUC). Optimal cutoff values were determined using the Youden index.

Nomograms, calibration plots, ROC curves, decision curve analysis (DCA), and clinical impact curves (CICs) were constructed using R packages including rms, regplot, and rmda. Internal validation of discrimination and calibration was performed using bootstrap resampling with 1,000 iterations, as described previously.[21]

For model reproducibility, the intercept and beta coefficients of the final X-ray screening model were reported.

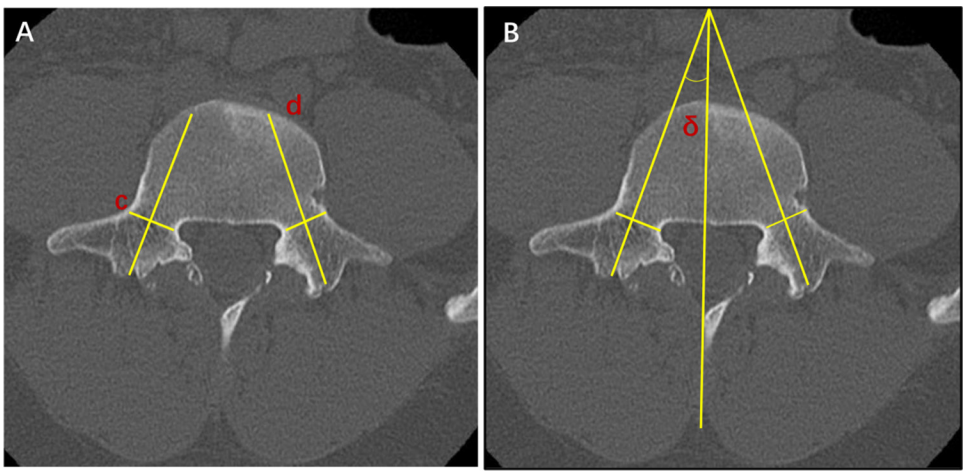


Figure 2. CT-based measurements. (A) Pedicle width (c) and intended screw depth (d). (B) Pedicle internal inclination angle (delta).

Multicollinearity among SI, SS, L5 LIA, and the L5 lumbar index was assessed using variance inflation factors (VIFs). Sensitivity analyses were performed by fitting the final X-ray model in the unmatched development cohort and in a subgroup without radiographic spondylolisthesis (grade 0). Threshold-based exploratory metrics included sensitivity, specificity, observed positive predictive value, observed negative predictive value, missed cases, and the proportion of patients classified below the threshold. Because PSM and case–control sampling alter disease prevalence, model-estimated probabilities, calibration, decision-analytic indices, and CT-reduction estimates were interpreted cautiously.

2.6. External validation

An independent external validation dataset was assembled from an independent tertiary referral center. Patients enrolled between January 2024 and January 2025 who underwent both standard lumbar radiography and lumbar CT within a defined time interval were screened. For external validation, a case–control dataset was constructed according to CT-confirmed outcome status and consisted of 200 patients, including 100 patients with L5 spondylolysis and 100 controls without pars interarticularis defects on CT.

The external validation dataset was entirely independent of the development dataset and was not involved in variable selection, model fitting, or threshold optimization. All variables required for the nomogram were complete, and no imputation was required. External validation followed a strict model-application-only approach: the original development-cohort regression coefficients were applied without modification, and no variable reselection, model refitting, or model updating was performed.

Because the external validation dataset was assembled using case–control sampling, external model performance was assessed primarily in terms of discrimination using the AUC, which is equivalent to the C-index for a binary outcome. Calibration, decision-analytic measures, positive and negative predictive values, and CT-reduction estimates in this setting were considered exploratory and sample-specific and were not used as the primary basis for model validation.

3. Results

3.1. Study population and propensity score matching

After screening, 151 eligible patients were included in the development dataset. Before PSM, the spondylolysis and control groups differed significantly in age ($p = 0.017$) and hypertension prevalence ($p = 0.034$), whereas sex, BMI, and diabetes mellitus did not differ significantly between groups.

Following 1:1 PSM, 114 patients were included in the matched cohort, with 57 patients in each group. Baseline demographic and clinical characteristics were well balanced after matching (Table 1). Measurement reliability was excellent, with ICCs ranging from 0.855 to 0.959 across all radiographic and CT-based parameters.

3.2. Radiographic and morphological comparisons

In the matched cohort, univariable analysis demonstrated that patients with L5 spondylolysis had significantly larger SS, L5 LIA, and pedicle internal inclination angle, as well as significantly smaller SI, IJS, and L5 lumbar index values than controls (Table 2).

Multivariable logistic regression further identified smaller SI and L5 lumbar index, together with larger SS, L5 LIA, and pedicle internal inclination angle, as factors independently associated with L5 spondylolysis (Table 2). These associations should not be interpreted as evidence of temporal or causal effects.

Table 1

Baseline characteristics before and after propensity score matching.

Characteristic	Control (*n* = 82)	Spondylolysis (*n* = 69)	*p*	Control (*n* = 57)	Spondylolysis (*n* = 57)	*p*
Age, mean ± SD, year	52.41 ± 13.03	46.45 ± 17.18	0.017	50.46 ± 12.68	50.77 ± 14.93	0.900
Sex, *n* (%)			0.225			0.850
Male	39 (47)	38 (55)		31 (54)	29 (51)	
Female	43 (53)	31 (45)		26 (46)	28 (49)	
Diabetes mellitus, *n* (%)			0.484			0.810
Yes	12 (15)	9 (13)		11 (20)	9 (16)	
No	70 (85)	60 (87)		46 (80)	48 (84)	
Hypertension, *n* (%)			0.034			0.440
Yes	20 (24)	8 (11)		11 (20)	7 (12)	
No	62 (76)	61 (89)		46 (80)	50 (88)	
BMI category, kg/m^2, *n* (%)			0.211			0.510
< 18.5	3 (3)	1 (1)		3 (5)	1 (2)	
18.5–23.9	25 (30)	31 (45)		19 (34)	24 (42)	
24–30	45 (55)	28 (41)		28 (49)	23 (40)	
> 30	9 (12)	9 (13)		7 (12)	9 (16)	

BMI = body mass index, PSM = propensity score matching, SD = standard deviation.

Table 2

Univariable and multivariable analyses of factors associated with L5 spondylolysis.

Variable	Control (*n* = 57)	Spondylolysis (*n* = 57)	Univariable *p*	OR	95% CI lower	95% CI upper	Multivariable *p*
SI	43.40 ± 8.16	40.59 ± 6.80	0.041	0.834	0.744	0.934	0.002
SS	35.77 ± 8.10	39.56 ± 7.97	0.011	1.166	1.035	1.314	0.011
L3 LIA	108.54 ± 3.63	107.21 ± 4.92	0.184				
L4 LIA	110.19 ± 4.21	111.53 ± 5.13	0.158				
L5 LIA	115.40 ± 5.44	127.14 ± 9.02	< 0.001	1.230	1.106	1.367	< 0.001
L3 IJS	48.20 ± 4.17	46.55 ± 3.64	0.028	1.045	0.805	1.356	0.740
L4 IJS	45.04 ± 3.37	43.68 ± 4.02	0.021	0.971	0.711	1.324	0.850
L5 IJS	39.85 ± 4.45	36.70 ± 5.73	0.001	1.046	0.860	1.272	0.655
Pedicle internal inclination angle	20.78 ± 4.96	24.47 ± 4.32	< 0.001	1.264	1.088	1.468	0.002
Intended screw depth	45.16 ± 4.87	45.58 ± 4.92	0.648				
Pedicle width	15.39 ± 2.76	15.23 ± 2.60	0.759				
L5 lumbar index (per 0.1-unit increase)	0.88 ± 0.09	0.80 ± 0.08	< 0.001	0.371	0.153	0.898	0.028

CI = confidence interval, IJS = intervertebral joint space, LIA = lamina inclination angle, OR = odds ratio, SI = sacral inclination angle, SS = sacral slope angle.

3.3. Diagnostic performance of individual radiographic parameters

ROC analysis was performed to evaluate the discriminative ability of individual radiographic parameters. L5 LIA demonstrated the strongest discrimination, with an AUC of 0.879 (95% CI, 0.813–0.944). This was followed by the L5 lumbar index (AUC = 0.771), SS (AUC = 0.637), and SI (AUC = 0.611) (Fig. 3).

3.4. Development and internal validation of the nomogram

Based on the multivariable analysis and the need to maintain an X-ray-only tool, the final screening nomogram incorporated the L5 lumbar index, SI, SS, and L5 LIA (Fig. 4). CT-based pedicle internal inclination angle was analyzed separately as a morphological feature and was not included in the nomogram. The final logistic equation was: $\text{logit}(p) = -12.415 - 0.151 \times \text{SI} + 0.114 \times \text{SS} + 0.194 \times \text{L5 LIA} - 10.673 \times \text{L5 lumbar index}$, where p represents the model-estimated probability of bilateral L5 spondylolysis in the study sample.

The VIFs for SI, SS, L5 LIA, and the L5 lumbar index were 1.66, 1.85, 1.47, and 1.25, respectively, indicating no substantial multicollinearity. Internal validation using bootstrap resampling demonstrated good model performance. The bootstrap-corrected concordance index was 0.911, and ROC analysis of the nomogram yielded an AUC of 0.916 (95% CI, 0.865–0.967), indicating strong discriminative ability. DCA and CIC analysis showed greater apparent net benefit than individual parameters within the development sample (Fig. 5), but these decision-analytic findings should be interpreted cautiously because matching alters the underlying prevalence.

At the development-cohort Youden threshold of 0.623, the X-ray screening model showed a sensitivity of 0.789 and specificity of 0.912, with 12 missed cases among 57 CT-confirmed cases and 56.1% of patients classified below the threshold. In sensitivity analyses, the model retained strong discrimination in the

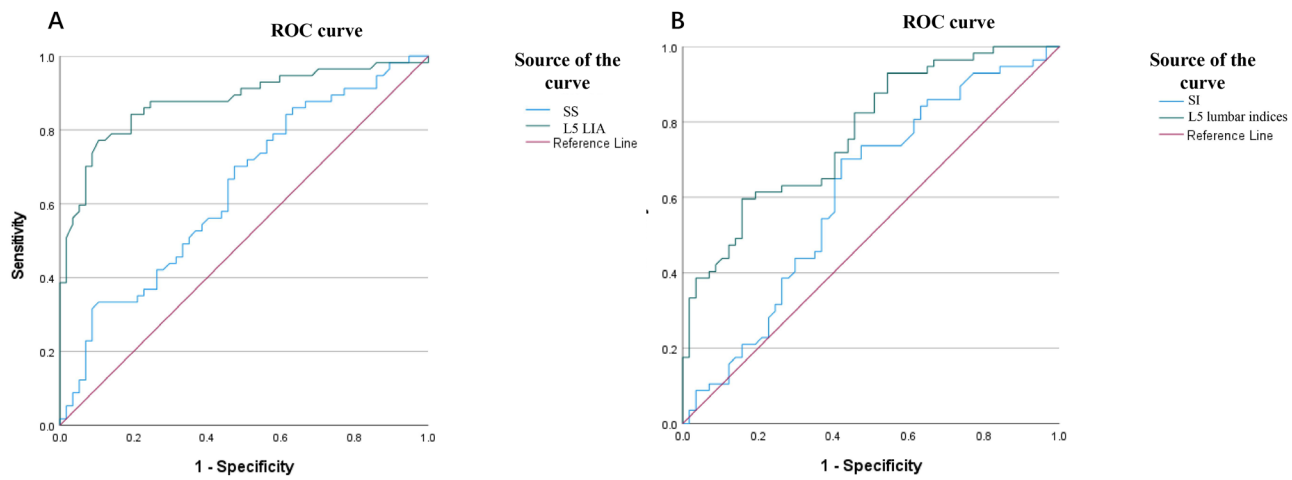


Figure 3. Receiver operating characteristic curves of individual radiographic parameters for L5 spondylolysis. (A) Sacral slope (SS) and L5 lamina inclination angle (L5 LIA). (B) Sacral inclination (SI) and L5 lumbar index. L5 LIA = L5 lamina inclination angle; SS = sacral slope.

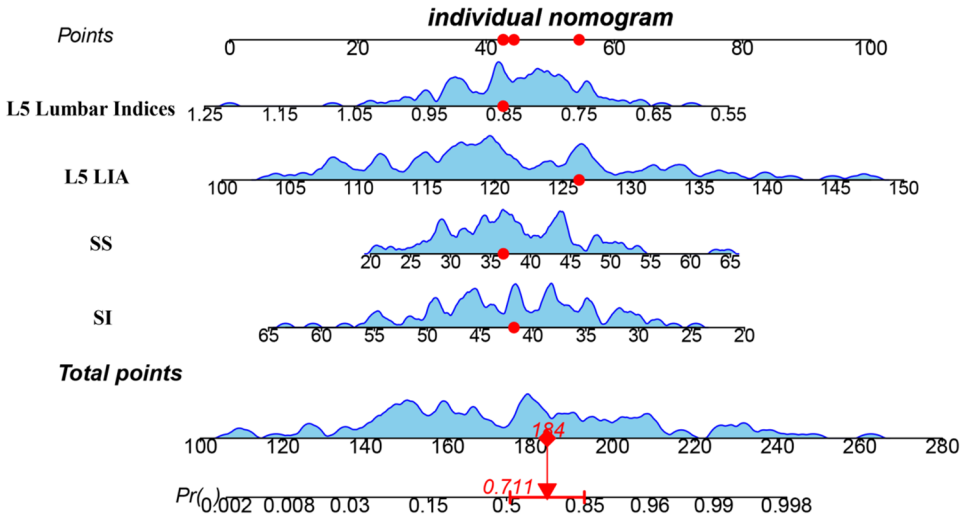


Figure 4. X-ray screening nomogram for bilateral L5 spondylolysis based on the L5 lamina inclination angle (L5 LIA), sacral slope (SS), sacral inclination (SI), and L5 lumbar index. L5 LIA = L5 lamina inclination angle; SI = sacral inclination; SS = sacral slope.

unmatched development cohort (AUC = 0.927; 95% CI, 0.885–0.968) and in the subgroup without radiographic spondylolisthesis (grade 0; AUC = 0.896; 95% CI, 0.806–0.986).

3.5. External validation results

The external validation dataset consisted of 200 patients from an independent institution, including 100 patients with CT-confirmed L5 spondylolysis and 100 controls. All variables required for the nomogram, including L5 LIA, SI, SS, and L5 lumbar index, were complete, and no missing data were identified (Fig. 6).

In the external validation dataset, the nomogram demonstrated strong discriminative performance when the original development-cohort coefficients were applied without refitting. ROC analysis yielded an AUC of 0.949 (95% CI, 0.922–0.977). Because the outcome was binary,

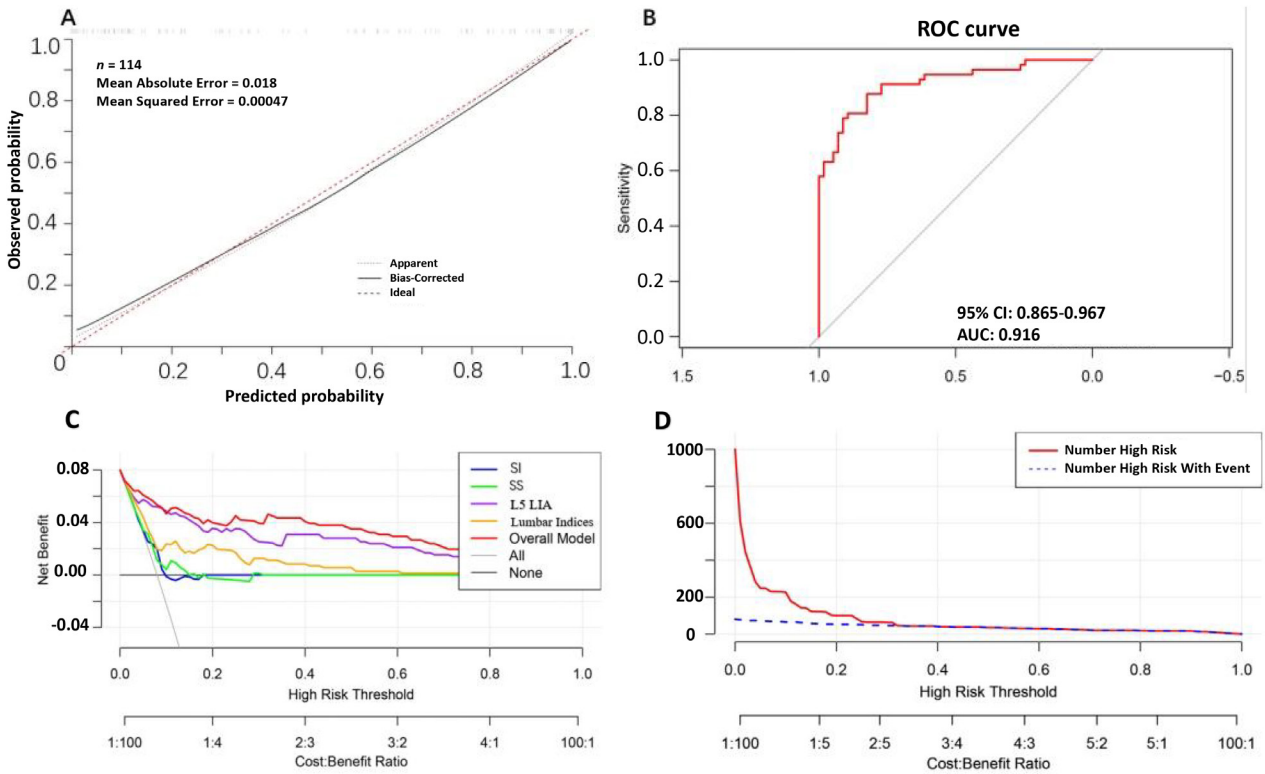


Figure 5. Internal validation of the X-ray screening nomogram. (A) Calibration plot of the nomogram in the development cohort. The diagonal dashed line represents perfect agreement, and the solid line represents the observed calibration of the model. (B) Receiver operating characteristic curve of the nomogram (AUC = 0.916; 95% CI, 0.865–0.967). (C) Decision curve analysis (DCA). (D) Clinical impact curve (CIC).

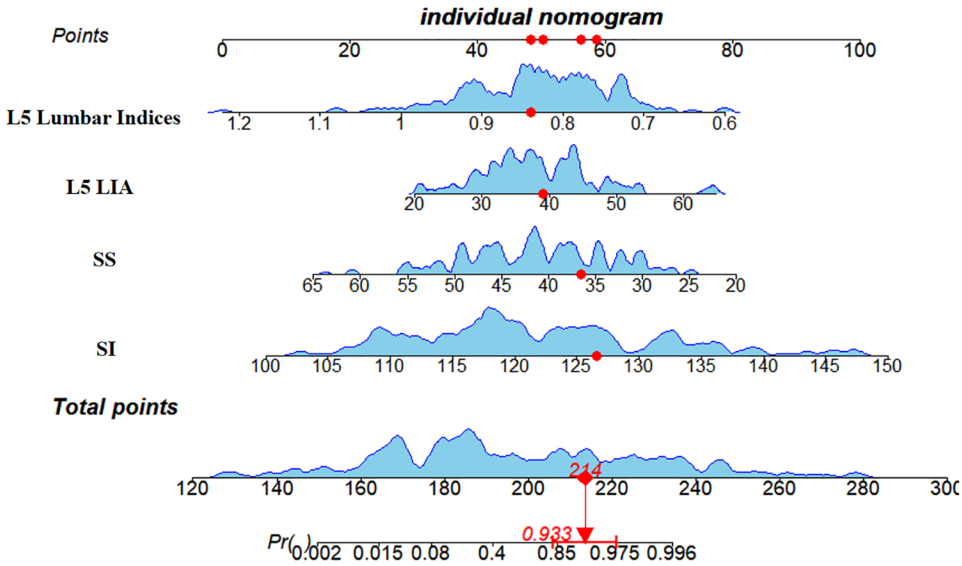


Figure 6. Example of individual radiographic risk stratification in the external validation dataset. The nomogram integrates the L5 lumbar index, L5 lamina inclination angle (L5 LIA), sacral slope (SS), and sacral inclination (SI). For a given patient, each parameter contributes a specific number of points, the sum of which corresponds to the model-estimated probability of bilateral L5 spondylolysis in the study sample. L5 LIA = L5 lamina inclination angle; SI = sacral inclination; SS = sacral slope.

the C-index was identical to the AUC (0.949), indicating the strong ability of the model to distinguish patients with L5 spondylolysis from controls in an independent external dataset.

At the development-cohort Youden threshold of 0.623, the external dataset showed a sensitivity of 0.830 and specificity of 0.910, with 17 missed cases among 100 CT-confirmed cases and 54.0% of patients classified below the threshold. At a lower threshold of 0.20, sensitivity increased to 0.970, specificity was 0.570, three cases were missed, and 30.0% of patients were classified below the threshold. These threshold-based estimates are exploratory because the external validation dataset used case–control sampling and therefore does not represent the disease prevalence or CT-use patterns of an unselected clinical population. Exploratory calibration and decision-analytic plots are shown in Figure 7 for descriptive completeness only and were not used as primary external validation endpoints.

4. Discussion

This study evaluated LIA as a radiographic marker associated with bilateral L5 spondylolysis. Patients with L5 spondylolysis had significantly larger L5 LIA values than controls, consistent with prior findings.[22] This phenomenon may be attributable to altered pedicle-facet geometry and mechanical loading at the pars interarticularis; however, the present cross-sectional design cannot determine whether these features precede the pars defect or represent adaptive remodeling after spondylolysis has developed. Biomechanical studies have shown that bilateral pars defects increase motion at L5–S1 while altering kinematics at adjacent segments, supporting the possibility that compensatory adaptations may occur away from the defect site.[23–25]

The surgical implications are also noteworthy. Anatomical distortion due to osteophyte formation and pseudoarthrosis may complicate pedicle screw placement, and navigation technologies have been developed to improve screw placement accuracy in challenging anatomy.[26,27] In the present study, patients with L5 spondylolysis had a significantly larger pedicle internal inclination angle. This finding should be interpreted as an associated morphological difference and potential adaptive consequence rather than a proven causal risk factor, but it may still be useful during preoperative planning.

Alterations in pelvic sagittal parameters play a critical role in spinal loading.[28–32] Increased sacral slope has been associated with spondylolisthesis progression, whereas lower SI and related sacral table morphology have been linked to spondylolysis risk.[33–37] These findings are consistent with the present results and underscore the biomechanical relevance of spinopelvic alignment in L5 spondylolysis.

Radiographic diagnosis of spondylolysis remains challenging, with limited sensitivity even when oblique views are added.[38–41] The nomogram developed in this study integrates readily obtainable radiographic parameters to provide individualized screening and risk stratification. Clinically, this model may help identify patients who warrant CT confirmation, but it should be used as a triage aid rather than as a replacement for CT when a definitive diagnosis is clinically required. Any claim regarding the reduction of unnecessary CT examinations requires prospective validation in consecutive clinical populations.

This study has several limitations. First, its cross-sectional design precludes causal inference; therefore, the radiographic and CT-based variables should be interpreted as associated features rather than proven

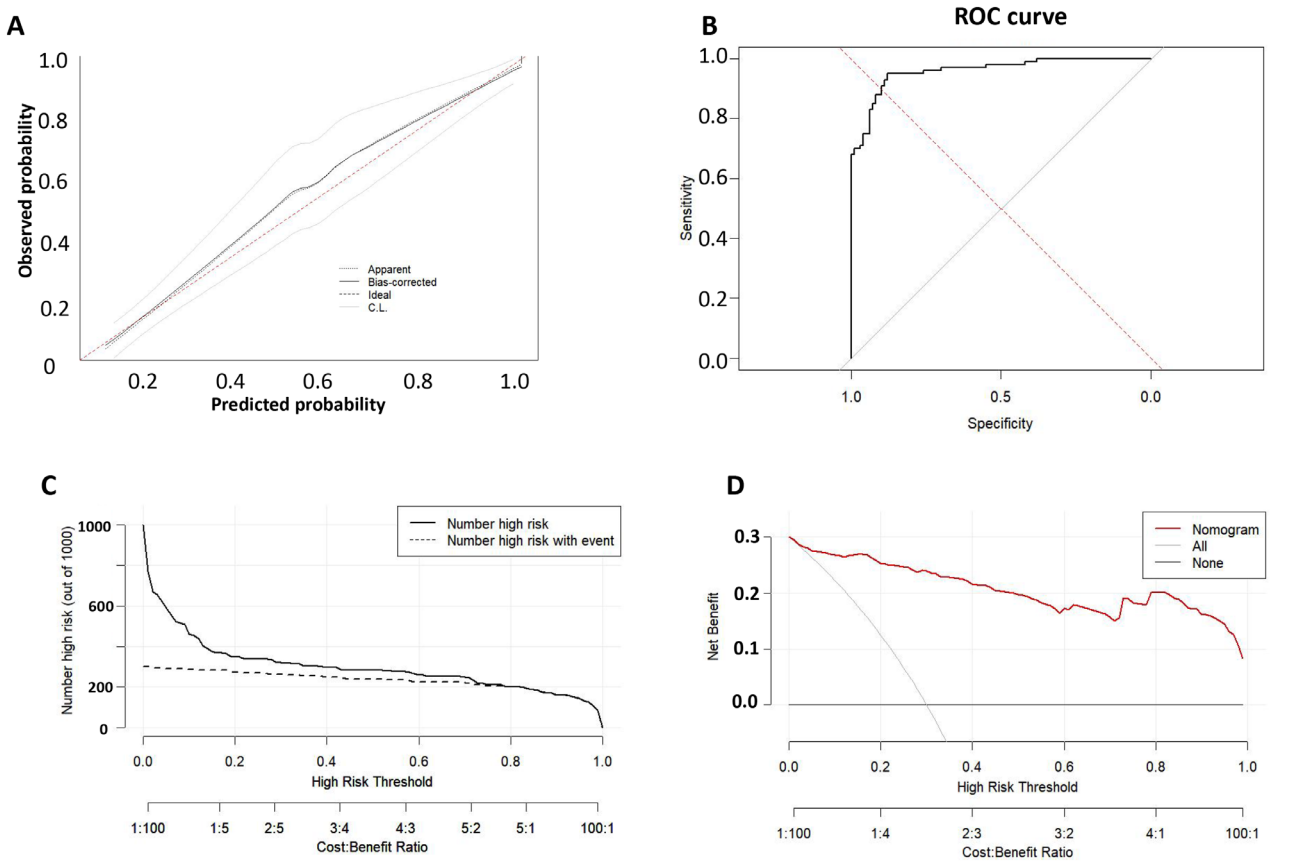


Figure 7. External validation of the X-ray screening nomogram in an independent case-control dataset. (A) Exploratory calibration plot shown for descriptive completeness only; because the external validation dataset used case-control sampling, this panel was not interpreted as a primary validation endpoint. (B) Receiver operating characteristic curve of the nomogram in the external validation dataset, demonstrating strong discriminative performance after application of the development-cohort coefficients without refitting (AUC = 0.949; 95% CI, 0.922–0.977). (C) Exploratory clinical impact curve (CIC) shown for descriptive completeness only. (D) Exploratory decision curve analysis shown for descriptive completeness only. Panels A, C, and D should be interpreted descriptively rather than as confirmatory external validation evidence. ROC = receiver operating characteristic curve.

etiologic risk factors. Second, only bilateral L5 spondylolysis was included. This restriction reduced heterogeneity and matched the intended model target, but it limits generalizability to unilateral, multilevel, or non-L5 spondylolysis. Third, PSM created a balanced analytical cohort but also altered the natural disease prevalence, limiting interpretation of model-estimated probabilities, calibration, positive and negative predictive values, and clinical utility. Fourth, although external validation was performed in an independent institution, the external validation dataset was assembled using a case-control sampling framework rather than a naturally occurring clinical cohort. Therefore, external validation primarily supports the discriminative performance of the model, whereas calibration, decision-analytic results, and possible reduction of CT use should be interpreted with caution. Fifth, spondylolisthesis may influence sagittal parameters and local morphology. Although sensitivity analysis in patients without radiographic spondylolisthesis showed preserved discrimination, future studies should prospectively evaluate the influence of spondylolisthesis severity and dynamic lumbar instability in consecutive populations.

5. Conclusions

This study identified key radiographic and morphological features associated with bilateral L5 spondylolysis and developed an X-ray-based screening nomogram for radiographic risk stratification. By integrating LIA, SI, SS, and the L5 lumbar index, the model demonstrated strong discriminative performance in the development cohort and retained strong discriminative performance in an independent external dataset when the original development-cohort coefficients were applied without refitting.

The proposed nomogram is a noninvasive, low-cost, and readily applicable radiographic screening aid for bilateral L5 spondylolysis. Its clinical role should be considered supportive: it may help stratify patients for further imaging evaluation, but definitive diagnosis and any CT-reduction strategy require prospective validation in consecutive clinical cohorts.

Acknowledgements

We express our sincere gratitude to the editor and reviewers for their constructive comments and to the journal and its publisher for their professional support.

Ethical statement

This study was approved by the Institutional Review Board and Ethics Committee of The Seventh Affiliated Hospital, Sun Yat-sen University, Shenzhen, China (Approval No. KY-2025-563-01, Date: December 10, 2025). The requirement for informed consent was waived by The Medical Ethics Committee of The Seventh Affiliated Hospital of Sun Yat-sen University. All procedures were conducted in accordance with applicable institutional guidelines and the Declaration of Helsinki.

Conflicts of interest

The authors declare that they have no conflicts of interest.

Funding source

This work was supported by the Shenzhen Key Laboratory of Bone Tissue Repair and Translational Research (No. ZDSYS20230626091402006) and the Sanming Project of Medicine in Shenzhen (Nos. SZSM202411014 and SZSM201911002) and the Shenzhen Strategic Emerging Industries Support Plan (No. XMHT20240115001).

Data availability statement

The datasets generated and/or analyzed during the current study are available from the corresponding author on reasonable request.

Author contributions

CC and FW—conceptualization.
CC—methodology.
XL and DH—investigation.
CC and XL—data curation.
CC and XL—formal analysis.
CC, HX, and JL—resources.
CC—writing – original draft.
CC, HX, JL, and FW—writing – review and editing.
HX and JL—revision according to editorial comments.
FW—supervision.
FW—funding acquisition.

References

[1] Mohile NV, Kuczmarski AS, Lee D, Warburton C, Rakoczy K, Butler AJ. Spondylolysis and isthmic spondylolisthesis: a guide to diagnosis and management. *J Am Board Fam Med*. 2022;35:1204–16.
[2] Lan Z, Yan J, Yang Y, Xu Q, Jin Q. A review of the main classifications of lumbar spondylolisthesis. *World Neurosurg*. 2023;171:94–102.
[3] Berger RG, Doyle SM. Spondylolysis 2019 update. *Curr Opin Pediatr*. 2019;31:61–8.
[4] Onal MB, Bahadir S. Bilateral spondylolysis of inferior articular processes of lumbar vertebra with no active sports history: case report and review of literature. *Br J Neurosurg*. 2023;37:334–6.
[5] Aoki Y, Takahashi H, Nakajima A, et al. Prevalence of lumbar spondylolysis and spondylolisthesis in patients with degenerative spinal disease. *Sci Rep*. 2020;10:6739.
[6] Li J, Liang J, Xu Y, et al. Incidence of lumbar spondylolysis in athletes with low back pain: a systematic evaluation and single-arm meta-analysis. *Medicine (Baltim)*. 2023;102:e34857.
[7] Mushtaq R, Porrino J, uzmán Pérez-Carrillo GJ. Imaging of spondylolysis: the evolving role of magnetic resonance imaging. *PM R*. 2018;10:675–80.
[8] Asai R, Tatsumura M, Gamada H, et al. Epidemiological differences between the sexes in adolescent patients with lumbar spondylolysis: a single-institution experience in Japan. *BMC Musculoskelet Disord*. 2023;24:558.
[9] Nakayama T, Ehara S. Spondylolytic spondylolisthesis: various imaging features and natural courses. *Jpn J Radiol*. 2015;33:3–12.
[10] Chung CC, Shimer AL. Lumbosacral spondylolysis and spondylolisthesis. *Clin Sports Med*. 2021;40:471–90.
[11] Foreman P, Griessenauer CJ, Watanabe K, et al. L5 spondylolysis/spondylolisthesis: a comprehensive review with an anatomic focus. *Childs Nerv Syst*. 2013;29:209–16.
[12] Song B, You SK, Lee JE, Lee SM, Cho HH. Prevalence of incidentally detected spondylolysis in children. *Taehan Yongsang Uihakhoe Chi*. 2022;83:127–37.
[13] Madhavan A, Siripurapu R, Herwadkar A. Imaging of juvenile spinal disorders. *Clin Radiol*. 2023;78:484–96.
[14] Huang Y, Dong Y, Liu F, Li Y, Wang H, Zhang J. Bilateral spondylolysis of lumbar vertebra secondary to long spinal fusion for idiopathic scoliosis: a case report and review of literature. *Orthop Surg*. 2024;16:2569–73.
[15] Exposito Jimenez D, Alvarez De Sierra Garcia B. Magnetic resonance imaging (MRI) vs. computed tomography (CT) in the diagnosis and classification of spondylolysis and spondylolisthesis—a narrative review. *Quant Imaging Med Surg*. 2024;14:7891–907.
[16] Song M, Sun K, Li Z, et al. Stress distribution of different lumbar posterior pedicle screw insertion techniques: a combination study of finite element analysis and biomechanical test. *Sci Rep*. 2021;11:12968.
[17] Xue C, Yuan J, Lo GG, et al. Radiomics feature reliability assessed by intraclass correlation coefficient: a systematic review. *Quant Imaging Med Surg*. 2021;11:4431–60.
[18] Koo TK, Li MY. A guideline of selecting and reporting intraclass correlation coefficients for reliability research. *J Chiropr Med*. 2016;15:155–63.
[19] Kane LT, Fang T, Galetta MS, et al. Propensity score matching: a statistical method. *Clin Spine Surg*. 2020;33:120–2.
[20] Zibugu D, Gubbels JS, Namugenyi C, Asiimwe JB, Gerards S. Impact of the timed and targeted counselling model on maternal health continuum of care outcomes in Northern Uganda: protocol of a quasi-experimental study. *Methods Protoc*. 2024;7:98.
[21] Asher AL, Devin CJ, Archer KR, et al. An analysis from the quality outcomes database, part 2: predictive model for return to work after elective surgery for lumbar degenerative disease. *J Neurosurg Spine*. 2017;27:370–81.
[22] Kong Q, Wei B, Niu S, Liao J, Zu Y, Shan T. Age, pelvic incidence, facet joint angle and pedicle-facet angle as correlative factors for isthmic spondylolisthesis: a retrospective case control study. *BMC Musculoskelet Disord*. 2023;24:497.
[23] Haj-Ali R, Wolfson R, Masharawi Y. A patient specific computational biomechanical model for the entire lumbosacral spinal unit with imposed spondylolysis. *Clin Biomech (Bristol)*. 2019;68:37–44.
[24] Pan J, Chen C, Liu C, Chou P. Biomechanical effects of a novel pedicle screw W-type rod fixation for lumbar spondylolysis: a finite element analysis. *Bioengineering (Basel)*. 2023;10:451.
[25] Sterba M, Arnoux P, Labelle H, Warner WC, Aubin CE. Biomechanical analysis of spino-pelvic postural configurations

in spondylolysis subjected to various sport-related dynamic loading conditions. *Eur Spine J*. 2018;27:2044–52.
[26] Viana SL, Viana MA, de Alencar EL. Atypical, unusual, and misleading imaging presentations of spondylolysis. *Skeletal Radiol*. 2015;44:1253–62.
[27] Dennler C, Jaberg L, Spirig J, et al. Augmented reality-based navigation increases precision of pedicle screw insertion. *J Orthop Surg Res*. 2020;15:174.
[28] Tartara F, Garbossa D, Armocida D, et al. Relationship between lumbar lordosis, pelvic parameters, PI-LL mismatch and outcome after short fusion surgery for lumbar degenerative disease: literature review, rationale, and presentation of public study protocol. *World Neurosurg X*. 2023;18:100162.
[29] Mazurek M, Kulesza B, Golebiowska N, Tyzo B, Kura K, Szczepanek D. Factors predisposing to the formation of degenerative spondylolisthesis-a narrative review. *Medicina (Kaunas)*. 2023;59:1430.
[30] Matsuzawa K, Matsui T, Azuma Y, et al. Spine alignment in standing and maximal upper limb elevation in baseball players with lumbar spondylolysis and those without low back pain. *Int J Environ Res Public Health*. 2023;20:3231.
[31] Kieffer WKM, Don A, Field A, Robertson PA. Lordosis loss in degenerative spinal conditions. *Spine Deform*. 2022;10:1407–14.
[32] Yin J, Peng BG, Li YC, Zhang NY, Yang L, Li DM. Differences of sagittal lumbosacral parameters between patients with lumbar spondylolysis and normal adults. *Chin Med J (Engl)*. 2016;129:1166–70.
[33] Abelin-Genevois K. Sagittal balance of the spine. *Orthop Traumatol Surg Res*. 2021;107:102769.
[34] Vrtovec T, Janssen MM, Likar B, Castelein RM, Viergever MA, Pernus F. A review of methods for evaluating the quantitative parameters of sagittal pelvic alignment. *Spine J*. 2012;12:433–46.
[35] Ru N, Luk KDK, Sun J, Wang G. The correlation of sacral table angle to spinopelvic sagittal alignment in healthy adults. *J Orthop Surg Res*. 2023;18:314.
[36] Sugawara K, Iesato N, Katayose M. Comparison of the sacral table angles by progression stage of lumbar spondylolysis. *Spine Deform*. 2020;8:123–7.
[37] Strube P, Pumberger M, Sonnow L, et al. Association between lumbar spinal degeneration and anatomic pelvic parameters. *Clin Spine Surg*. 2018;31:263–7.
[38] Saremi A, Goyal KK, Benzel EC, Orr RD. Evolution of lumbar degenerative spondylolisthesis with key radiographic features. *Spine J*. 2024;24:989–1000.
[39] Fraiwan M, Audat Z, Fraiwan L, Manasreh T. Using deep transfer learning to detect scoliosis and spondylolisthesis from x-ray images. *PLoS One*. 2022;17:e0267851.
[40] Saifuddin A, White J, Tucker S, Taylor BA. Orientation of lumbar pars defects: implications for radiological detection and surgical management. *J Bone Joint Surg Br*. 1998;80:208–11.
[41] Miller R, Beck NA, Sampson NR, Zhu X, Flynn JM, Drummond D. Imaging modalities for low back pain in children: a review of spondylolysis and undiagnosed mechanical back pain. *J Pediatr Orthop*. 2013;33:282–8.

How to cite this article: Chan C, Liu X, He D, Xiang H, Li J, Wei F. A novel X-ray-based screening model for bilateral L5 spondylolysis. *Spine Res*. 2026;2(3):173–182. doi: 10.1097/br9.0000000000000039